Surface barrier energies on strontium titanate

R. C. Neville and C. A. Mead

Citation: Journal of Applied Physics **43**, 4657 (1972); doi: 10.1063/1.1660984
View online: http://dx.doi.org/10.1063/1.1660984
View Table of Contents: http://scitation.aip.org/content/aip/journal/jap/43/11?ver=pdfcov
Published by the AIP Publishing

[28]G. Shachar, S. Mardix, and I. T. Steinberger, J. Appl. Phys. **39**, 2485 (1968).
[29]J. Tauc, Rev. Mod. Phys. **29**, 308 (1957).
[30]J. Tauc and M. Závětová, Czech. J. Phys. **9**, 572 (1959).
[31]G. Shachar, Y. Brada, E. Alexander, and Y. Yacobi, J. Appl. Phys. **41**, 723 (1970).
[32]I. B. Kobyakov and G. S. Pado, Sov. Phys. Solid State **9**, 1707 (1968).
[33]A. Von Hippel, Z. Phys. **133**, 158 (1952).
[34]P. Provetto, V. Maxia, and C. Muntoni, Nuovo Cimento B **69**, 219 (1970).
[35]R. Scarmozzino, Solid State Commun. **9**, 1159 (1971).
[36]O. Brafman, E. Alexander, B. S. Fraenkel, Z. H. Kalman, and I. T. Steinberger, J. Appl. Phys. **35**, 1855 (1964).

Surface barrier energies on strontium titanate

R. C. Neville
Department of Electrical Engineering, University of California, Santa Barbara, California 93106

C. A. Mead
Department of Electrical Engineering, California Institute of Technology, Pasadena, California 91109
(Received 28 April 1972)

The metal-semiconductor surface-barrier systems consisting of the metals gold, palladium, copper, or indium on chemically prepared or cleaved strontium titanate surfaces have been investigated in detail. Surface-barrier energies have been studied by photoresponse, forward current versus voltage, and thermal activation energy techniques yielding values in excellent agreement with each other. Forward current-voltage characteristics were in quantitative agreement with simple diode thermionic theory as modified by the inclusion of image force lowering. The reverse current-voltage characteristic of these stable barriers also is in agreement with that expected from thermionic theory including simple image force lowering over a bias range from -0.1 to -4 V.

INTRODUCTION

Known for only a relatively few years, strontium titanate is becoming increasingly important as a synthetic gem stone and, in combination with barium titanate, as the dielectric material in high-value capacitors.[1] More importantly, strontium titanate is a member of the peroskvite family of compounds with a wide spectrum of basic physical and electrical properties, ranging from superconduction to semiconduction. Strontium titanate is of cubic structure at room temperature[2] consisting of a titanium atom at the center of the cube, oxygen atoms on the faces, and strontium atoms in the corners. As the temperature is decreased, the crystal structure shifts to tetragonal at 110 °K, orthorhombic at 65 °K, and there exists evidence for a shift to the rhombohedral at 10 °K.[2]

Electrically, the pure crystal is an insulator with a room-temperature forbidden band gap of 3.15 eV.[3] At temperatures above 65 °K the pure single-domain material exhibits a dielectric constant consistent with a Curie temperature of 30 °K.[4] Below 65 °K the relative permittivity increases smoothly, but neither multiple-domain[5] nor single-domain[4] samples become ferroelectric above 4.2 °K.

Upon reduction by heating in a hydrogen atmosphere, the clear colorless insulating crystal becomes a semiconductor of a varying shade of blue as the result of free carrier absorption.[6] At low temperatures (less than 1 °K) strontium titanate crystals exhibit superconductivity.[7] At temperatures between 4.2 and 300 °K there have been a number of mobility studies[8–12] with noticable variation in observed values of mobility. The surface-barrier energies of metals on strontium titanate have received scant attention,[13] and present values of the surface-barrier energies are uncertain.

To understand a semiconductor, it is essential that the surface-barrier properties of metals on that semiconductor be known. A systematic investigation of the surface-barrier properties of gold, palladium, copper, and indium surface barriers on both chemically prepared and on cleaned strontium titanate surfaces was conducted. The techniques of photoresponse, forward current-voltage charactersitic, and thermal activation energy were employed. Values of surface-barrier energy as measured by these methods were found to be in good agreement. Additionally, forward and reverse current-voltage characteristics were studied and analyzed in terms of simple Bethe diode theory[14] as modified by image force lowering.

SAMPLE PREPARATION

Two clear colorless boules of strontium titanate with resistivity in excess of 10^{11} Ω cm were used. The boules, obtained from the National Lead Co., were grown using the same process but a year apart in time.[1] Using a diamond saw, the boules were sliced into wafers 1.5 mm thick in a direction parallel to the (100) faces. Two wafers were cut from each 100-carat boule. The four wafers were hand lapped and polished on a succession of silk cloths starting with an 800-mesh grit, progressing through 1200 and 3200 grits, 1- and 0.3-μ polishing compounds, and finishing with a 500-Å alumina polishing compound. Final wafer thickness was approximately 1 mm.

The four wafers were sliced into 12 sample bars whose dimensions were approximately $1\times2\times10$ mm. Bars 1—6 come from boule A and bars 7—12 come from boule B. These bars were cleaned by etching in phosphoric acid for 10 min, followed by immersion in hydrochloric acid for 10 min. After a 15-min rinse in flowing deionized water, the 12 bars were dried in a jet of dry filtered air.

One bar from each boule was tested for resistivity by soldering leads on each of the two small ends and two

TABLE I. Preparation parameters, bulk resistivity, and mobility measurements on typical strontium titanate samples.

Sample bar	1,11	2,7	3,12	5,10	6,8	Units
			Preparation			
Temperature	770	750	750	795	830	°C
Atmosphere	1.5	1.5	1.5	1.5	1.5	psi hydrogen
Time	240	180	10	240	420	min
			300 °K electrical values[a]			
Resistivity	11.8	27.1	39.6	1.36	0.30	Ω cm
Mobility	7.35	8.85	8.95	26	31.8	cm^2/V sec
Electron concentration	7.15	3.1	2.0	17.0	66.0	10^{16} cm^{-3}

[a]Values determined to ± 5% accuracy.

more leads along one long side of the rectangular bar. Using a four-point method, the resistivity was confirmed to be in excess of 10^{11} Ω cm for both boules. To determine the purity of the material and confirm the information furnished with the boules by the manufacturer, National Lead Co., sample bars No. 4 and No. 9 were submitted to the Geology Department of the California Institute of Technology for an impurity analysis. There, Dr. A. Chodos performed a semiquantitative analysis using an electron microprobe. Principal impurities found were 0.0002% barium, 0.01% calcium oxide, and less than 0.1% tungsten. These data are in agreement with those furnished by the manufacturer.

The remaining sample bars were recleaned on an individual basis and placed in a purified hydrogen furnace at a pressure of 1.5 psi and heated to temperatures between 750 and 830 °C for periods of time between 10 min and 7 h. This process created oxygen vacancies which acted as donors[13] in sufficient quantities to yield electron concentrations between 2×10^{16} and 7×10^{17} cm^{-3}. The crystal bars, as a result of free carrier absorption,[6] now range in color from a pale blue to almost black.

Leads were soldered to the sample bars using a low-temperature melting, 10% silver—90% indium, solder, and Hall and resistivity measurements were made at room temperature. The results obtained are listed in Table I. Note that similar preparation procedures yield similar results on the two boules.

Next, the samples' surface layers were removed by soaking for 10 min in hydrochloric acid, to remove solder, 10 min at 50 °C in phosphoric acid, and 10 min in hydrochloric acid. The samples were rinsed in deionized water for 15 min and dried in a jet of dry filtered air. Gold, palladium, copper, or indium barriers were evaporated through a fine screen onto the polished chemically prepared surface in an ion-pumped vacuum with a nominal pressure of 5×10^{-7} Torr. Nominal barrier diameter was 100 μ. Two leads were soldered to the bulk of each sample bar using a 90% indium—10% silver solder, and a contact made to the barrier by a gold wire held in a micromanipulator. After electrical measurements had been made, each sample bar was again placed in a vacuum of 5×10^{-7} Torr nominal pressure. Each sample was vacuum cleaved in a stream of evaporating gold, palladium, copper, or indium. Barrier area and sample lead configuration were similar to the chemically prepared surface samples.

SURFACE-BARRIER MEASUREMENTS

The properties of gold, palladium, copper, and indium surface barriers on both chemically prepared and on cleaved strontium titanate surfaces were investigated. Barrier energies were determined using photoresponse, current-voltage characteristics, and thermal activation energy techniques. The surface-barrier energies as obtained by these methods were found to be consistent.

PHOTORESPONSE

The surface-barrier energy was determined by a measurement of the short-circuit photocurrent using light entering the crystal from the barrier contact surface (a front-wall configuration). A tungsten-halide lamp was used in conjunction with a Gaertner quartz-prism monochrometer. The light was chopped at 50 Hz, and a lock-in amplifier was used to improve the signal-to-noise ratio. From simple Fowler theory,[15] the barrier energy is the intercept for zero current of the plot of the square root of the response (photocurrent per incident photon) versus the photon energy.

In Fig. 1 we present the typical photoresponse data for gold, palladium, copper, and indium surface barriers on chemically prepared strontium titanate surfaces. In Fig. 2 we present typical data for these metals on cleaved strontium titanate surfaces. The photoresponse data on both chemically prepared and cleaned surfaces

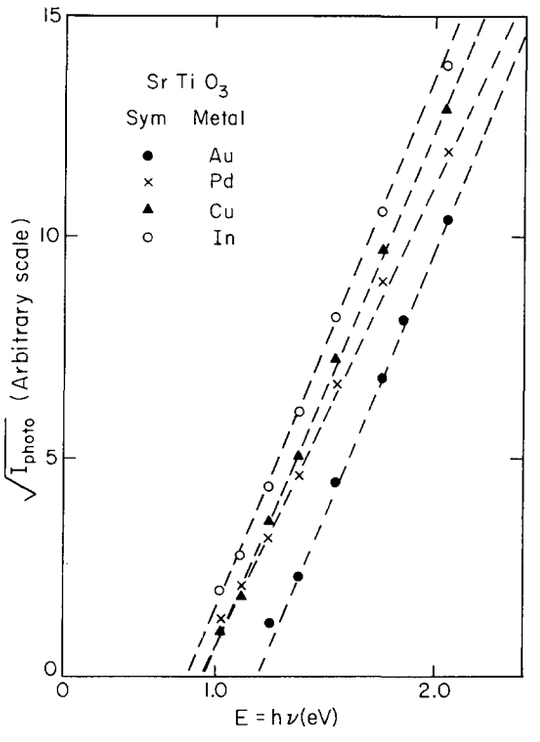

FIG. 1. Square root of the photo current per photon vs photon energy for surface barriers on chemically prepared strontium titanate surfaces at 300 °K.

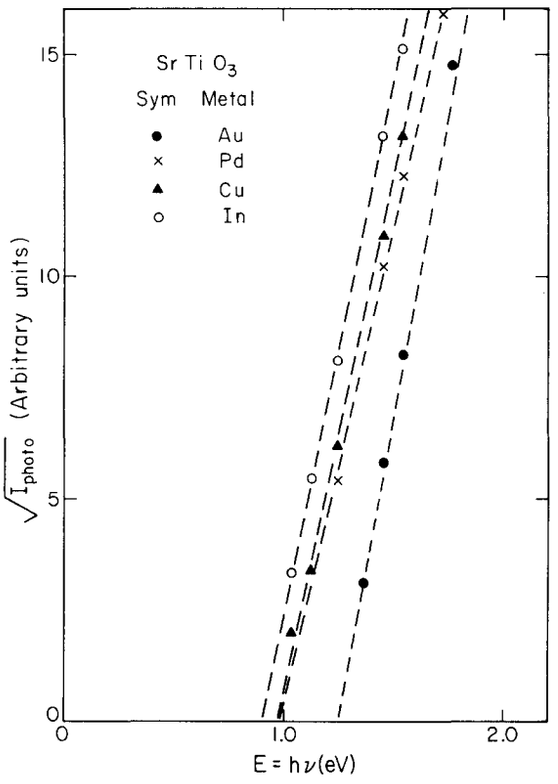

FIG. 2. Square root of the photo current per photon for surface barriers on vacuum-cleaved strontium titanate surfaces at 300°K.

is linear in accord with theory.[15] At high photon energies, surface scattering and impurity absorption act to reduce the response below that expected from simple theory. To determine the effects of electron concentration on barrier energy, several sample bars were tested for each type of metal barrier. Sample bars 1—3, 6—8, 11, and 12 were used for gold barriers, 1, 3, 5, and 10—12 for palladium barriers, 5—8 and 10 for copper surface barriers, and 5, 6, and 10 for indium surface barriers. No indication of any effect of carrier concentration was observed. Surface-barrier energies as determined by photoresponse were in agreement for samples from the two boules. The data presented in Table II represent an average of the 60—80 devices measured.

FORWARD CURRENT—FORWARD VOLTAGE

Typical curves of the logarithm of the forward current density versus forward voltage are presented in Fig. 3 for gold, palladium, copper, and indium on chemically prepared surfaces and in Fig. 4 for the same metals on vacuum-cleaved strontium titanate surfaces. The individual surface-barrier areas were nominally 8×10^{-5} cm^2, and the same samples were used as in the photoresponse measurements to facilitate comparison of measurements. Currents were applied by a battery and variable resistor or a Keithly 225 current source. Voltages were measured with a Darcy 440 digital voltmeter and a Keithly 163 digital voltmeter. All measurements were made in darkness to eliminate effects of light-stimulated generation-recombination current. Two bulk contacts were used in a three lead configuration to minimize parasitic resistance effects.

The current-voltage characteristic, for thermionic current and voltages in excess of a few kT/q is given by (see Appendix A):

$$J = J_0 \exp(qv/nkT), \tag{1}$$

where J is the current density, v is the applied voltage, k is the Boltzmann constant, T is the absolute temperature, n is the diode nonideality factor, and

$$J_0 = A^* T^2 \exp(-q\phi_B/nkT), \tag{2}$$

where ϕ_B is the time surface-barrier energy, A^* is the Richardson constant corresponding to the effective mass of the charge carriers:

$$A^* = m^* qk^2/2\pi^2\hbar^3, \tag{3}$$

where m^* is the effective mass, taken as $16m_e$ after Kuhn and Leyendecker.[16] m_e is the rest mass of the free electron and $\hbar$ is Planck's constant divided by 2π. From Eq. (2) it is clear that the surface-barrier energy can be determined by extrapolation of the high current voltage characteristic to zero applied voltage:

$$\phi_B = \frac{nkT}{q} \ln \frac{A^* T^2}{J_0} . \tag{4}$$

In Figs. 3 and 4, the straight-line behavior of the logarithm of the current density as a function of applied voltage over three orders of current magnitude is in excellent agreement with thermionic theory [Eq. (1)]. The effect of excess series resistance can be seen at high current levels, and the reverse current component decreases the observed forward current at small forward voltage levels. The slope of the log current versus voltage is experimentally observed to be 63.7 ± 1.5 mV per decade of current. This corresponds to a value of n equal to 1.07 ± 0.03. Using this value and the observed extrapolated zero-voltage current intercepts, the values of surface-barrier energy listed in Table II for both chemically prepared and cleaved surfaces were determined. The energies given represent an average of the 60—80 barriers measured.

THERMAL ACTIVATION ENERGY

The third measurement of surface-barrier energy was obtained from the measurement of reverse current as a function of temperature with a fixed-bias voltage. The

TABLE II. Surface-barrier energies (eV) on strontium titanate.

Technique	Photo-response	*I-V* characteristic	Activation energy	Average
		Chemically prepared surface		
Gold	1.20 ± 0.06	1.16 ± 0.05	1.22 ± 0.06	1.19 ± 0.06
Palladium	0.94 ± 0.04	0.97 ± 0.05	1.01 ± 0.05	0.97 ± 0.05
Copper	0.95 ± 0.05	0.89 ± 0.04	0.95 ± 0.05	0.93 ± 0.04
Indium	0.87 ± 0.03	0.86 ± 0.025	0.87 ± 0.04	0.87 ± 0.03
		Cleaved surface		
Gold	1.25 ± 0.03	1.17 ± 0.07	1.26 ± 0.08	1.23 ± 0.07
Palladium	0.98 ± 0.02	1.02 ± 0.05	1.05 ± 0.04	1.02 ± 0.04
Copper	0.97 ± 0.03	0.92 ± 0.04	0.97 ± 0.02	0.95 ± 0.03
Indium	0.90 ± 0.022	0.90 ± 0.013	0.90 ± 0.022	0.90 ± 0.02

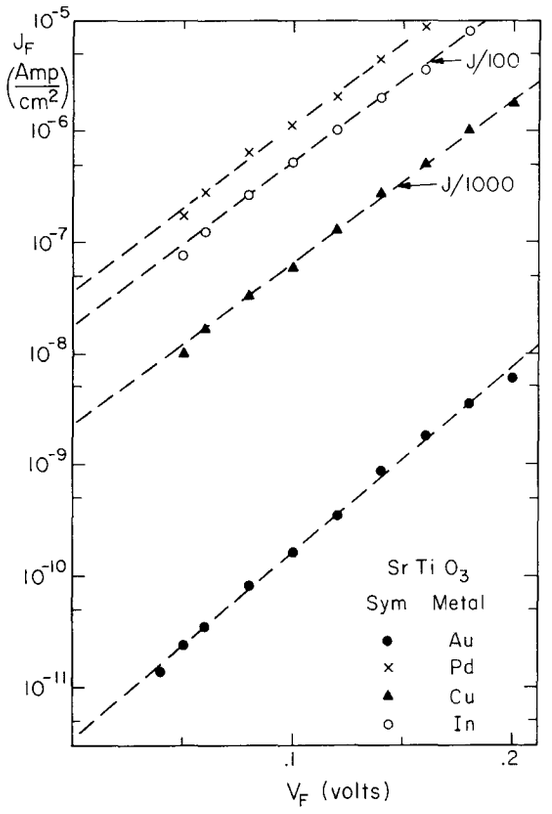

FIG. 3. Logarithm of the forward current density vs voltage for surface barriers on chemically prepared strontium titanate surfaces at 300 °K.

surface barriers were biased at -1 V using a battery-operated power supply. The measurements were made using a Keithly 602 electrometer and a Darcy 440 digital voltmeter. Temperature variation was obtained using a Peltier cooler-heater, and the measurements were made in the dark to minimize generation-recombination current.

Typical values of the logarithm of the normalized reverse current versus inverse temperature are given in Fig. 5 for gold, palladium, copper, and indium surface barriers on chemically prepared strontium titanate surfaces. Similar data for cleaved surfaces are presented in Fig. 6. (The observed current magnitudes of the reverse current at room temperature were in the 10^{-7}–10^{-12}-A range.) Repeatability of the measurements was ±2% with the exception of a 13 °C measurement on gold surface barriers and the 7 °C measurement on palladium surface barriers owing to the difficulty encountered in measuring the low currents involved in the latter two instances.

The thermal activation energy was obtained from the slope of the log current versus inverse temperature plot as expected from simple theory[14]:

$$\phi_A = \frac{k}{q}\left(\frac{\partial \ln I_s(v)}{\partial 1/T}\right) - \frac{2kT}{q}, \tag{5}$$

where ϕ_A is the thermal activation energy. The thermal activation energy determined from Eq. (5) is expected to be higher than the barrier energy, due to the change in barrier energy with temperature. The barrier energy can be expressed as[17]:

$$\phi_B = \phi_A + A_1 T, \tag{6}$$

where

$$A_1 = \frac{\partial \phi}{\partial T} = \frac{\phi}{E_g}\frac{\partial E_g}{\partial_T} < 0, \tag{7}$$

where E_g is the forbidden band gap.

The surface-barrier energies given in Table II, as measured by the thermal activation energy technique, were determined from the thermal activation energy using a forbidden gap of[3] 3.15 eV and a rate of change in the width of the gap with temperature of -9.5×10^{-4} eV/°K.[18] Agreement with the data from the other techniques is good.

REVERSE CURRENT MEASUREMENTS

Reverse current measurements were made in the dark with a battery and variable resistor power supply using an EGG picoammeter as a current meter. Temperature was held at 300 °K.

In Fig. 7 we present normalized data for the log reverse current versus α, where α is the fourth root of the barrier energy less Fermi level, temperature conversion kT/q, and applied voltage, for gold, palladium, copper, and indium surface barriers on cleaved strontium titanate surfaces. Also presented in Fig. 7 are

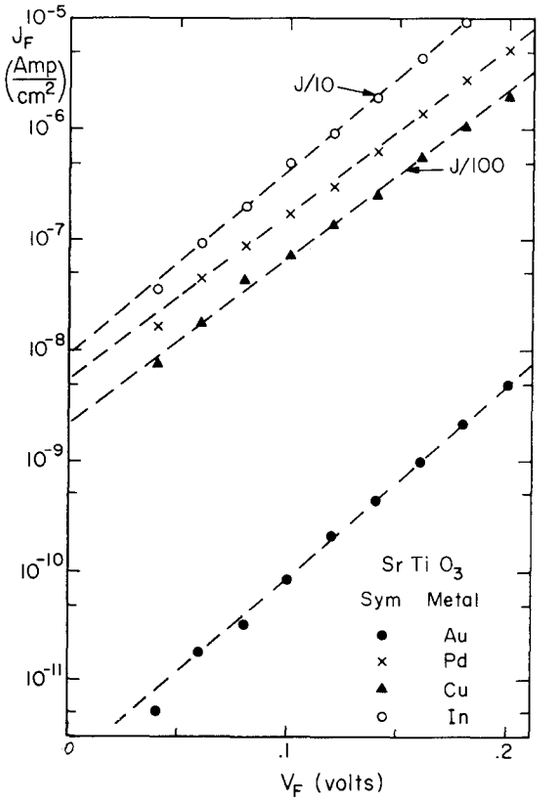

FIG. 4. Logarithm of the forward current density vs voltage for surface barriers on vacuum-cleaved strontium titanate surfaces at 300 °K.

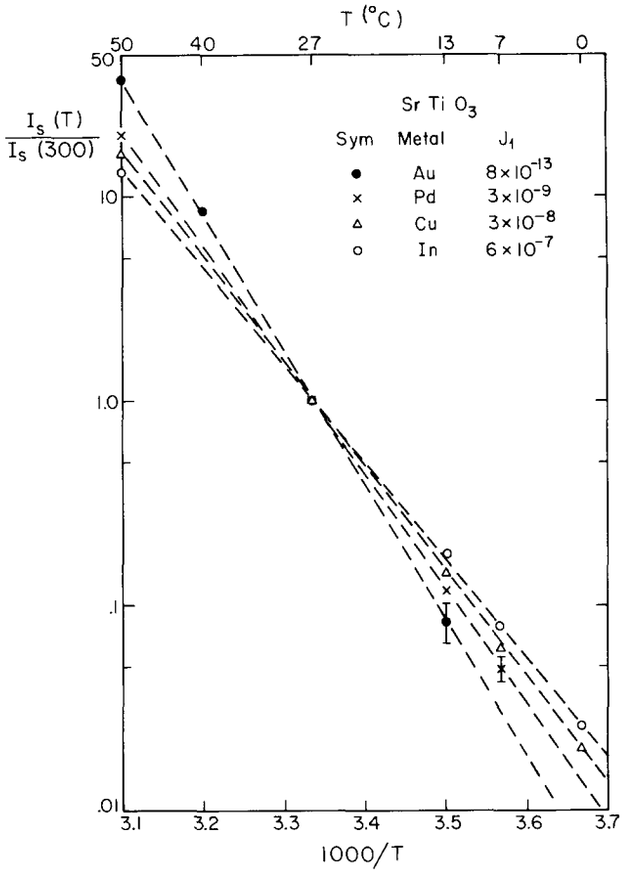

FIG. 5. Logarithm of the normalized reverse current vs inverse temperature for surface barriers on chemically prepared strontium titanate surfaces at −1 V bias.

theoretical curves of log reverse current versus α. From Bethe[14] diode theory and image force lowering (Appendices A and B), the logarithm reverse current is expected to vary with voltage as

$$\frac{\partial \ln I_s(v)}{\partial (v_0 - v)^{1/4}} = \left(\frac{q}{kT}\right)\left(\frac{q^3 N_D}{8\pi^2 \epsilon_0^3 \epsilon_{opt} 2\epsilon_r}\right)^{1/4}, \tag{8}$$

where I_s is the reverse current, v is less than zero, N_D is the donor density, ϵ_0 is the free space permittivity, ϵ_{opt} is the optical relative permittivity of strontium titanate, ϵ_r is the low-frequency permittivity of strontium titanate, and

$$v_0 = \phi_B - \xi - (kT/q) = \alpha + v, \tag{9}$$

where ξ is the Fermi level of the material. The theoretical curves were calculated using a unitary value of optical dielectric constant and a value[4] of 330 for the low-frequency relative permittivity.

Agreement between the theoretical approach and experiment is excellent both in slope and, for 80% of the barriers examined, in magnitude of the current.

DISCUSSION AND CONCLUSION

Gold, palladium, copper, and indium surface barriers on both cleaved and chemically prepared strontium titanate surfaces have been measured. Photoresponse, forward current-voltage, and thermal activation energy techniques have been used. The values obtained by these three independent methods are listed in Table II along with their average values. We find the surface-barrier energies on chemically prepared strontium titanate to be 1.19 ± 0.06 eV for gold, 0.97 ± 0.05 eV for palladium, 0.93 ± 0.04 eV for copper, and 0.87 ± 0.03 eV for indium. On cleaved strontium titanate surfaces the surface-barrier energies are 1.23 ± 0.07 eV for gold, 1.02 ± 0.04 eV for palladium, 0.95 ± 0.03 eV for copper, and 0.90 ± 0.02 eV for indium.

Each value represents an average of the mutually consistent values obtained by use of the three independent techniques of measurement. Each technique involved the measurement of 60—80 individual surface barriers. Approximately one-half of the surface barriers were taken from each boule. The uncertainty represented in Table II is equal to the maximum scatter in data points taken on individual barriers. The variation in surface-barrier energy on any single sample bar was equal to or greater than the variation between bars or boules. No consistent change of barrier energy was observed as a function of electron concentration. The slightly lower values of surface-barrier energy on chemically prepared surfaces is the result of surface states on the material[18] and has been seen elsewhere.[19]

For a purely ionic semiconductor the surface-barrier

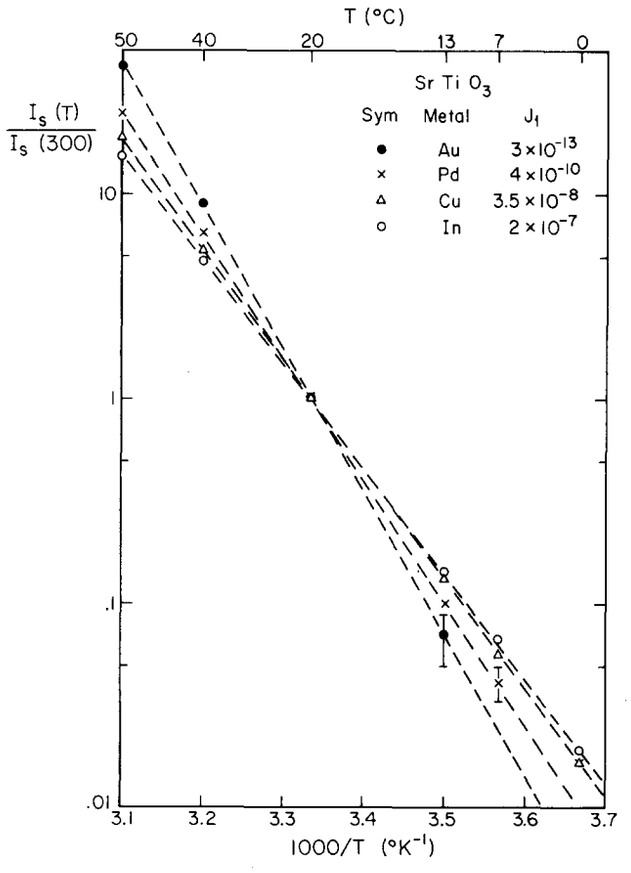

FIG. 6. Logarithm of the normalized reverse current vs inverse temperature for surface barriers on cleaved strontium titanate surfaces as a −1 V bias.

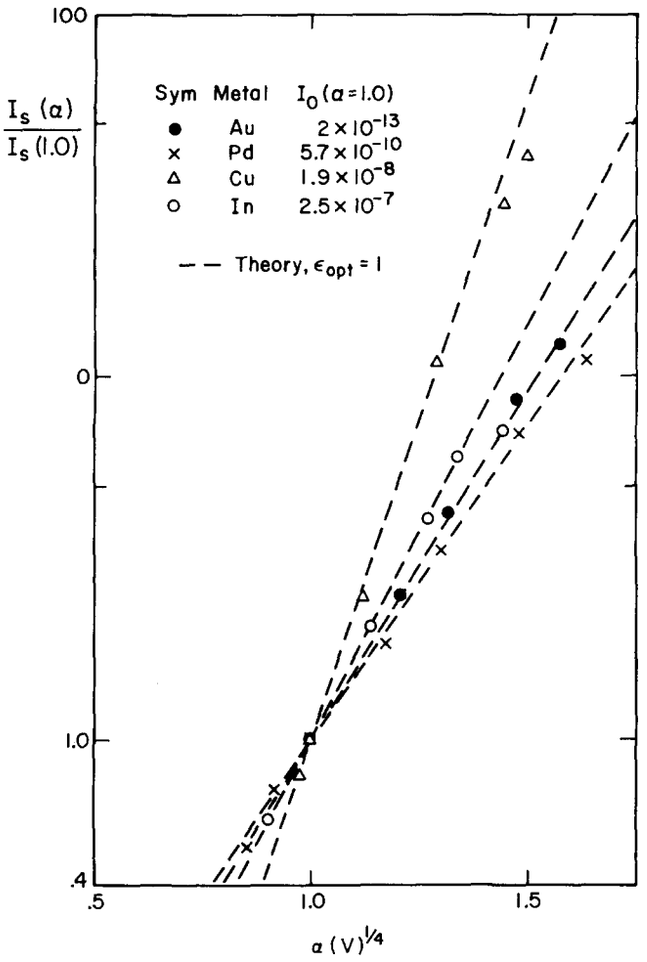

FIG. 7. Logarithm of the normalized reverse current vs α for surface barriers on cleaved strontium titanate at 300°K: $\alpha = [\phi_B - \xi - (kT/q) - V]^{1/4}$.

energy will track the metal electronegativity.[20,21] For a typical covalent semiconductor, the surface-barrier energy will be pinned by surface states and hence constant independent of the metal employed. Copper has an electronegativity of 1.9, indium 1.7, palladium 2.2, and gold has an electronegativity of 2.4. Study of the variation with metal of the surface-barrier energies obtained on strontium titanate indicates a mixed bonding scheme with ionic bonding being a major component.

The current-voltage characteristics in both forward and reverse directions follow simple thermionic diode theory as modified by the addition of image force lowering. The voltage dependence of both forward and reverse current is consistent with an optical dielectric constant of unity and with the observed values of effective mass[16] and dielectric constant.[14] The current magnitudes are in agreement with that predicted from theory over three orders of magnitude in both forward and reverse directions.

In conclusion, the surface-barrier energies of several metals on both chemically prepared and cleaved strontium titanate surfaces have been determined by several independent techniques. The observed properties of the barriers are consistent with simple diode theory as modified by image force lowering.

APPENDIX A: THERMIONIC FORWARD VOLTAGE–FORWARD CURRENT CHARACTERISTIC

For thermionic current the diode current is given by Bethe[14] as

$$J = J_0[\exp(qv/kT) - 1], \tag{A1}$$

$$J = A^*T^2 \exp(-q\phi/kT), \tag{A2}$$

$$A^* = (qm^*/2\pi^2\hbar^3)k^2. \tag{A3}$$

The effect of image for a lowering, a phenomonon considered in detail in Appendix B can be included by writing for the barrier energy ϕ:

$$\phi = \phi_B - \left(\frac{q^3N_D}{8\pi^2\epsilon_{opt}2\epsilon_r\epsilon_0^3}\right)^{1/4}\left(\phi_B - \xi - v - \frac{kT}{q}\right)^{1/4}$$
$$= \phi_B - \Delta\phi, \tag{A4}$$

where ϵ_0 is the relative permittivity of free space, ϵ_{opt} is the optical-frequency dielectric constant, ϵ_r is the low-frequency dielectric constant, ϕ_B is the barrier energy, N_D is the carrier impurity density, and ξ is given by

$$\xi = \frac{kT}{q}\ln\frac{N_C}{N_D}, \tag{A5}$$

where N_C is the conduction-band density of states. For voltages such that the exponential term in (A1) exceeds unity by a factor of ~10 or more

$$J = A^*T^2 \exp[(-q/kT)(\phi_B - \Delta\phi - v)]. \tag{A6}$$

Taking the logarithm to the base e,

$$\ln\frac{J}{A^*T^2} = -\frac{q\phi_B}{kT} + \frac{q\Delta\phi}{kT} + \frac{qv}{kT}. \tag{A7}$$

Differentiating and recalling that $\partial\Delta\phi/\partial v$, $\partial\Delta\phi/\partial\phi_B \ll 1$

$$\partial\ln\frac{J}{A^*T^2} = \frac{-q\,\partial\phi_B}{kT[1+(\partial\Delta\phi/\partial\phi)]} + \frac{q\,\partial v}{kT[1-(\partial\Delta\phi/\partial v)]} \tag{A8}$$

or

$$J = A^*T^2 \exp\left(\frac{-q\phi_B}{nkT}\right)\exp\left(\frac{qv}{nkT}\right), \tag{A9}$$

where

$$n = 1 + \frac{\partial\Delta\phi}{\partial(\phi_B - \xi - v)}. \tag{A10}$$

See also Sze[22] and Henish.[23]

APPENDIX B: IMAGE FORCE LOWERING

The metal side of a metal-semiconductor interface has a very high density of fixed charges in comparison to the semiconductor. Applying a reverse bias to such a Schottky barrier results in a depletion region, which to first order may be considered to extend solely into the semiconductor. Applying Gauss's law, and assuming a constant relative permittivity,

$$\nabla^2\phi = -p/\epsilon = -qN_D/\epsilon_r\epsilon_0, \tag{B1}$$

where ϕ is the potential, q is the electronic charge, N_D is the density of fixed donor atoms, ϵ_r is the low-fre-

quency dielectric constant, and ϵ_0 is the permittivity in vacuum. We take as a reference point the junction itself and set $\phi(0)=0$. The other important boundary condition is $E(X_D)=(-\partial\psi/\partial x)(X_D)=0$, where X_D is the maximum value of the depletion layer width and E is the electric field. Integrating,

$$\phi(X)=(qN_D/\epsilon_r\epsilon_0)(XX_D-\tfrac{1}{2}X^2). \tag{B2}$$

An electron approaching the energy barrier from the right (in the semiconductor) will see an image of itself. The force on the electron will be[22]

$$F=\frac{q^2}{4\pi\epsilon_{opt}\epsilon_0(2X)^2}=-q\nabla(\Delta\phi), \tag{B3}$$

where ϵ_{opt} is the optical dielectric frequency. Integrating,

$$\Delta\phi=q/16\pi\epsilon_{opt}\epsilon_0 X. \tag{B4}$$

The net potential in the depletion field region is given by

$$\phi(X)=\frac{qN_D}{\epsilon_0\epsilon_r}(XX_D-\tfrac{1}{2}X^2)+\frac{q}{16\pi\epsilon_{opt}\epsilon_0 X}. \tag{B5}$$

At some critical distance from the origin (junction), X_C, the image force potential results in an electric field strong enough to counterbalance the electric field produced by the built-in and applied bias. For $X<X_C$ the image force is dominant, while for $X>X_C$ the bias and built fields are the principal fields. At $X=X_C$ the field is zero and

$$0=\frac{qN_D}{\epsilon_r\epsilon_0}(X_D-X_C)-\frac{q}{16\pi\epsilon_{opt}\epsilon_0 X_C^2} \tag{B6}$$

from

$$\phi(X_D)=\phi_0-\xi-(kT/q)$$

and Eqs. (B2) and (B6)

$$\Delta\phi=\phi(X_C)=\left(\frac{q^3N_D}{8\pi^2\epsilon_{opt}^2\epsilon_r\epsilon_0^3}\right)^{1/4}\left(\phi_0-\xi-v-\frac{kT}{q}\right)^{1/4}. \tag{B7}$$

[1] M. D. Beals (private communication).
[2] F. W. Lytle, J. Appl. Phys. **35**, 2212 (1964).
[3] H. W. Gandy, Phys. Rev. **113**, 795 (1959).
[4] R. C. Neville, B. Hoeneisen, and C. A. Mead, J. Appl. Phys. **43**, 2124 (1972).
[5] R. C. Neville, B. Hoeneisen, and C. A. Mead, J. Appl. Phys. **43**, 3903 (1972).
[6] W. S. Baer, Phys. Rev. **144**, 734 (1966).
[7] C. S. Koonce and M. L. Cohan, Phys. Rev. **163**, 380 (1967).
[8] H. P. R. Frederiske and G. A. Candella, Phys. Rev. **147**, 583 (1966).
[9] H. P. R. Frederiske, W. R. Thurber, and E. R. Hosler, Phys. Rev. A **134**, 442 (1964).
[10] H. P. R. Frederiske and E. R. Hosler, Phys. Rev. **161**, 822 (1967).
[11] O. N. Tufte and P. W. Chapman, Phys. Rev. **155**, 799 (1967).
[12] C. Lee, J. Yahia, and J. L. Brebner, Phys. Rev. B **3**, 2525 (1971).
[13] J. E. Carnes and A. M. Goodman, J. Appl. Phys. **38**, 3091 (1967).
[14] M. A. Bethe, MIT Radiation Laboratory Report No. 43/12, 1966 (unpublished).
[15] R. H. Fowler, Phys. Rev. **38**, 45 (1931).
[16] A. H. Kuhn and A. J. Leyendecker, Phys. Rev. **135**, 134 (1964).
[17] W. Shockley, *Electrons and Holes in Semiconductors* (Van Nostrand, Princeton, N. J. 1950), pp. 267–270, 335, 520–531.
[18] A. M. Goodman, J. Appl. Phys. **34**, 329 (1963).
[19] R. C. Neville and C. A. Mead, J. Appl. Phys. **41**, 3795 (1970).
[20] R. C. Neville, thesis (California Institute of Technology, 1971) (unpublished).
[21] R. O. Bell and G. Rupprecht, Phys. Rev. **129**, 90 (1963).
[22] S. M. Sze, *Physics of Semiconductor Devices* (Interscience, New York, 1969), Chap. 8.
[23] H. K. Henish, *Rectifying Semiconductor Contacts* (Clarendon, Oxford, 1957).

Hot-electron concept for Poole-Frenkel conduction in amorphous dielectric solids*

J. Antula †

James Franck Institute and Department of Physics, The University of Chicago, Chicago, Illinois 60637

(Received 5 April 1972)

The general calculation of Poole-Frenkel conduction for amorphous solids must take into account the existence of Coulombic centers and a range of shallow trap centers. The hot-electron concept leads to the proper distribution of electrons between these traps and the conduction band in the presence of the applied electric field and at finite temperatures. Including the effect of hot electrons we achieve a better agreement between the theory and experimental data obtained with amorphous Al_2O_3, Ge, and SiO films.

I. INTRODUCTION

The Poole-Frenkel effect—thermal excitation of an electron over a field-lowered Coulombic barrier surrounding a positive local charge—is a bulk-limited electron emission. The nature of the electron injection from the metal contacts into the insulator has a negligible influence on it, as stated by Simmons[1] and Jonscher.[2]

Most amorphous solids at the electric fields in excess of 10^4 V/cm show a range of nonlinear current-voltage dependence, and in most cases this can be interpreted as Poole-Frenkel emission. This means that thin amorphous films as diverse as carbon,[3] germanium,[4–6] silicon,[5] and aluminum-,[7–9] nickel-,[10] niobium-,[11] silicon-,[12–16] tantalum-,[17] titanium-,[9] and zirconium-[18] oxide, and Teflon and Mylar[19] show a range of common conducting mechanism, even if the relative orders of magnitude of some physical parameters may vary in wide limits. Also one and the same substance may show different performances according to the preparation method. But typical for Poole-Frenkel emission is always the current independence of electrode material and of polarity of the applied bias.

In the electric field range mentioned above and over a wide range of temperatures it seems that Poole-Frenkel emission is the most common conducting mechanism for amorphous semiconducting and insulating materials, under the condition that the interelectrode distance is large in comparison with the electron path between two